https://doi.org/10.17952/37EPS.2024.P2294

A comprehensive structural study on AT1 Receptor Variants: Towards the Design of Potent Biased Agonists

Malihe Hassanzadeh[1], Audrey Collette[1], Brian Holleran[1], Stéphane Laporte[2,3], Richard Leduc[1], Pierre-Luc Boudreault[1*]

[1]Department of Pharmacology and Physiology, Faculty of Medicine & Health Sciences, University de Sherbrooke, Sherbrooke, Quebec J1H 5N4, Canada
[2]Department of Pharmacology and Therapeutics, McGill University, Montréal, Québec H3G 1Y6, Canada
[3]Department of Medicine, McGill University Health Center, McGill University, Montréal, Québec H4A 3J1, Canada

INTRODUCTION

The angiotensin II type 1 receptor (AT1R) is a crucial component of the renin-angiotensin system (RAS), which plays a significant role in regulating blood pressure, and cardiovascular health [1]. Biased agonism is an emerging concept that allows the activation of specific signaling pathways of G protein-coupled receptors (GPCRs). It involves selectively targeting the receptor with a ligand that stimulates one pathway while inhibiting others, leading to more precise treatments with fewer side effects. To gain a deeper understanding of GPCR functional selectivity at a molecular level, this study focuses on the use of AT1R mutants and biased agonists. The activation of the AT1R by different agonists leads to different signaling pathways which is known as functional selectivity [2]. Understanding this mechanism can help to develop more effective and targeted treatments for hypertension and other cardiovascular diseases. To assess the activation of Gq and the recruitment of β-arrestin in response to the stimulation of AT1R with angiotensin II (AngII), [Sar1Ile8], AngII [Sar1LBpa8]AngII, and [Sar1DBpa8]AngII ligands, we opted to substitute position W2536.48, also referred to as the rotamer toggle switch, with alanine (W253A-AT1R). The activation of Gq and recruitment of β-arrestin were quantified using BRET-based biosensors. Our results indicate that the mutant W253A-AT1R was able to activate Gq and recruit β-arrestin when stimulated with AngII. However, upon stimulation with [Sar1Ile8]AngII or [Sar1DBpa8]AngII, which are β-arrestin-biased ligands on AT1R, W253A-AT1R mutant failed to recruit β-arrestin. Interestingly, [Sar1LBpa8]AngII could activate β-arrestin in the W253A-AT1R mutant background.

HIT to LEAD DEVELOPMENT

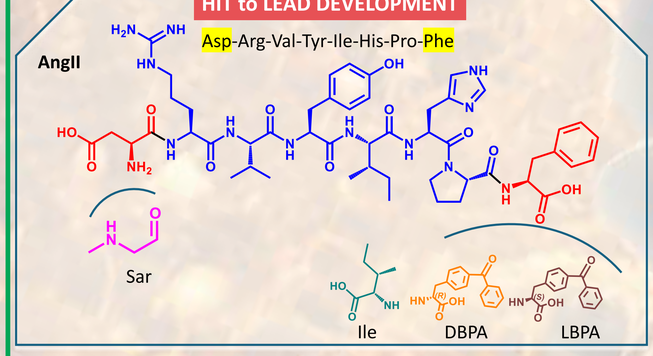

SAR STUDIES

Phe8: Alteration of the C-terminal F8 of AngII profoundly attenuates Gq-mediated signaling but not β-arrestin coupling.

Lack of an eighth residue, and an F8→A substitution, are deficient in Gq-dependent inositol phosphate generation.

Asp1: Protection against proteolytic degradation, and there is very little effect on activity.

BINDING ASSAY on the PEPTIDE LIGANDS

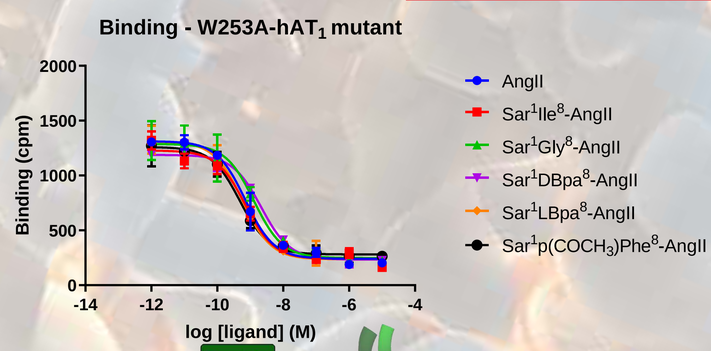

	AngII		[Sar¹Ile⁸]AngII		[Sar¹LBpa⁸]AngII		[Sar¹DBpa⁸]AngII	
	pIC50	*n*	pIC50	*n*	pIC50	*n*	pIC50	*n*
AT_1R	-9.25 ± 0.12	5	-9.02 ± 0.24	5	-9.33 ± 0.08	3	-8.41 ± 0.03	3
W253A	-9.10 ± 0.12	4	-8.82 ± 0.26	3	-9.45 ± 0.21	3	-8.72 ± 0.20	3
W253F	-8.72 ± 0.17	3	-9.24 ± 0.27	3	-9.10 ± 0.39	3	-8.41 ± 0.27	3

Figure 1. Binding properties of AngII analogues on AT_1R and mutant W253A-AT_1R. Dose-displacement binding curves was performed using ^{125}I-AngII and increasing amounts of indicated ligands. Binding affinities were determined as indicated in the accompanying table.

MOLECULAR MODELING STUDIES

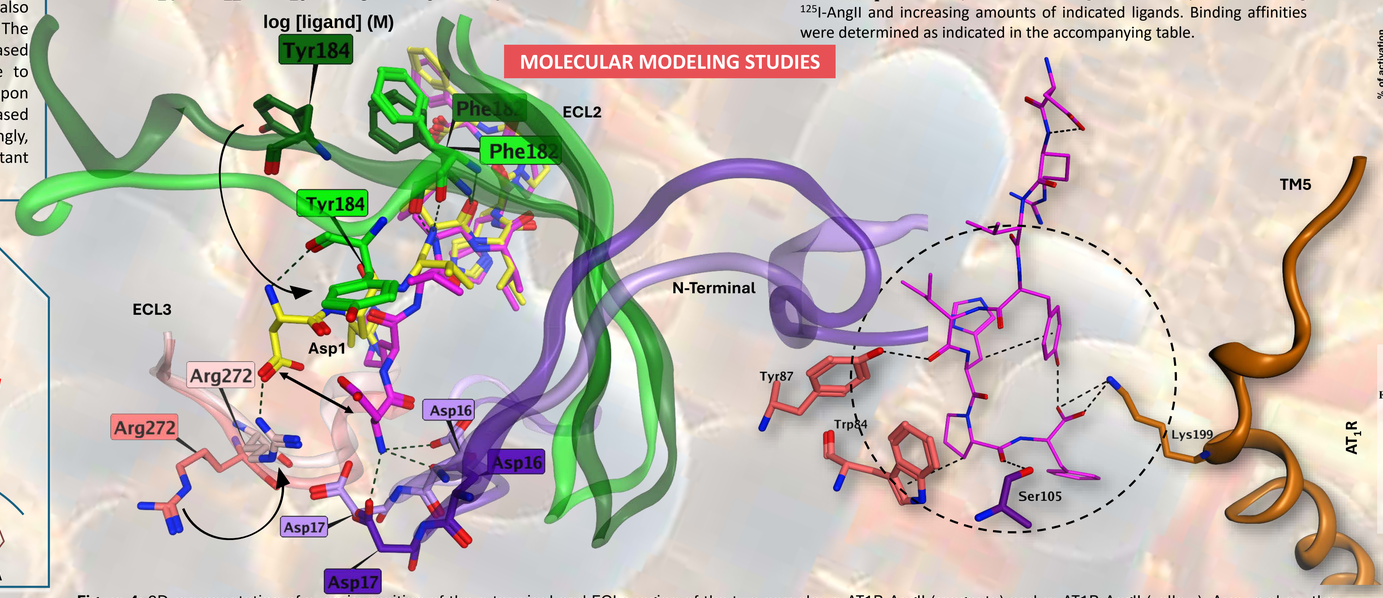

Figure 4: 3D representation of superimposition of the n-terminal and ECLs region of the two complex n-AT1R-AngII (magenta) and m-AT1R-AngII (yellow). Arrows show the conformational change after mutation in the regions (left). Cyclization through intramolecular interactions in AngII (P4 to P8) and interactios C-terminal and Lys199 (TM5).

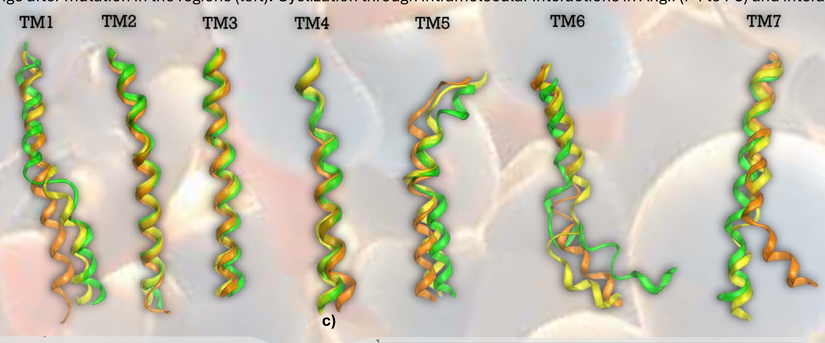

Figure 5: Superimposition of transmembrane helices (TMs) in the mutant AT1R complexes with different ligands. The TMs are shown for the m-AT1R complex with AngII (yellow), SLBPA (green), and SDBPA (orange). The image highlights the conformational differences and structural alignments of the TMs in the presence of different ligands, providing insights into how ligand binding affects the structural dynamics of the mutant receptor.

SIGNALING PROFILES of AT1R and MUTANT W253A

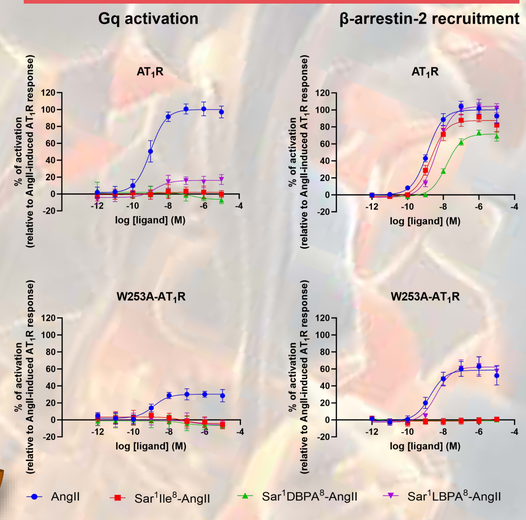

Figure 2. Signaling profiles of AT_1R and mutants induced by [Sar¹Ile⁸]AngII, [Sar¹DBpa⁸]AngII and [Sar¹LBpa⁸]AngII. AngII and indicated ligands induced Gq activation and b-arrestin-2 of AT_1R and W253A-AT_1R. HEK293 cells transfected with the indicated mutants and biosensor were stimulated with increasing concentration of AngII at room temperature.

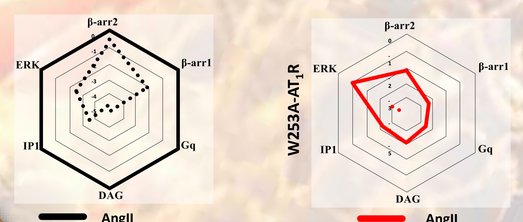

Figure 3. Effects of AngII and [Sar¹Ile⁸]AngII on AT_1R and AT_1R mutants signaling pathways. Radar graph representations summarizing the calculated $\Delta\log(\tau/K_A)$ values of the different ligand-activated pathways.

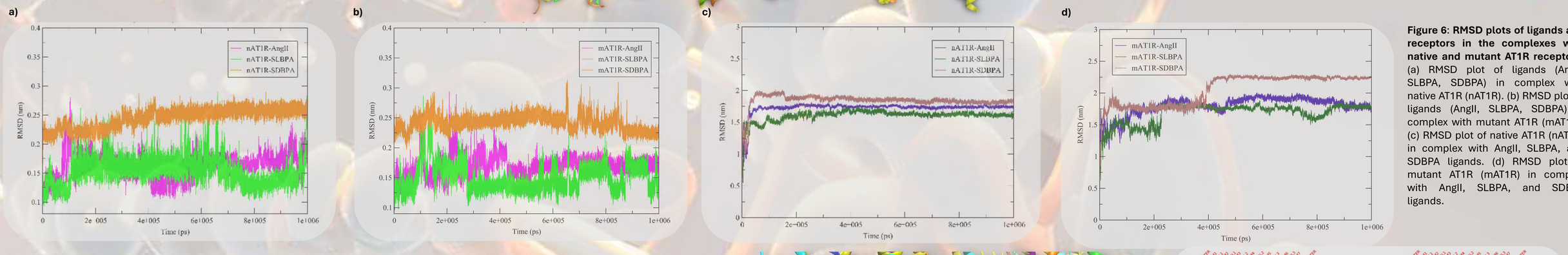

Figure 6: RMSD plots of ligands and receptors in the complexes with native and mutant AT1R receptors. (a) RMSD plot of ligands (AngII, SLBPA, SDBPA) in complex with native AT1R (nAT1R). (b) RMSD plot of ligands (AngII, SLBPA, SDBPA) in complex with mutant AT1R (mAT1R). (c) RMSD plot of native AT1R (nAT1R) in complex with AngII, SLBPA, and SDBPA ligands. (d) RMSD plot of mutant AT1R (mAT1R) in complex with AngII, SLBPA, and SDBPA ligands.

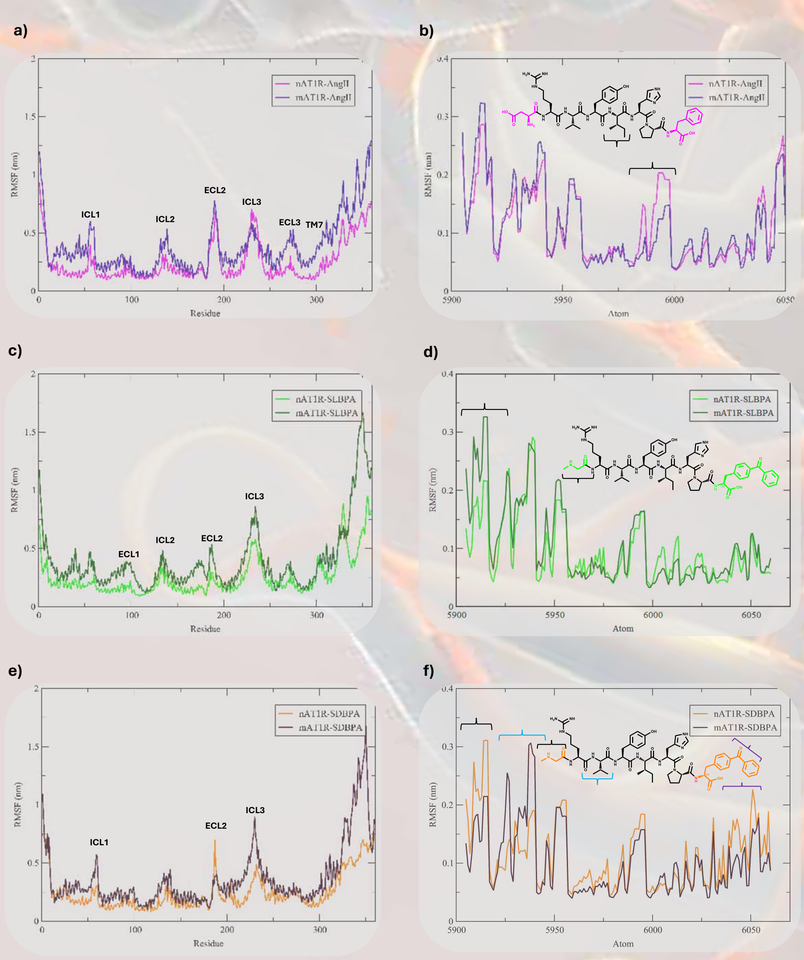

Figure 7: RMSF plots of AngII and AT1R receptors in complexes. (a) RMSF plot of native AT1R (nAT1R) and mutant AT1R (mAT1R) in complex with AngII. (b) RMSF plot of AngII in complex with native AT1R (nAT1R) and mutant AT1R (mAT1R). (c) RMSF plot of native AT1R (nAT1R) and mutant AT1R (mAT1R) in complex with SLBPA. (d) RMSF plot of SLBPA in complex with native AT1R (nAT1R) and mutant AT1R (mAT1R). In all the plots, RMSF of the ligands are plotted as a function of atom number and for the receptors as a function of residue number. (e) RMSF plot of native AT1R (nAT1R) and mutant AT1R (mAT1R) in complex with SDBPA. (f) RMSF plot of SDBPA in complex with native AT1R (nAT1R) and mutant AT1R (mAT1R).

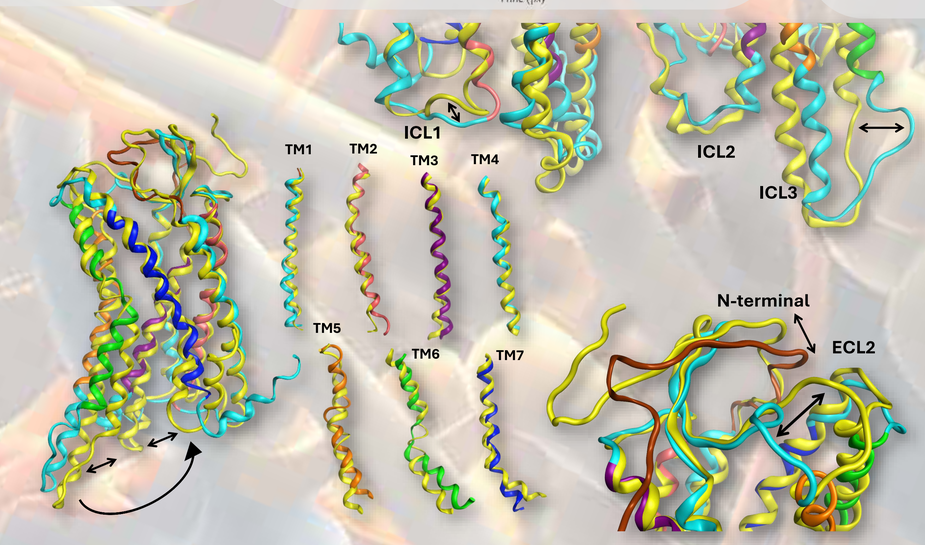

Figure 8. Comparative structural analysis of the nAT1R-SDBPA (cyan) and mAT1R-SDBPA (yellow) complexes highlighting the conformational changes upon mutation. The transmembrane helices (TMs) are color-coded as follows in the native receptor: TM2 (pink), TM7 (blue), TM6 (green), TM5 (orange), TM3 (magenta). Notable regions such as the N-terminal, ECL2, ICL1, ICL2, and ICL3 are labeled for clarity. Arrows indicate regions of significant conformational changes in the mutant complex.

Figure 9. Comparative structural analysis of the nAT1R (cyan)-SDBPA (orange) (left) and mAT1R (yellow)-SDBPA (orange) (right) complex interactions. The transmembrane helices (TMs) are color-coded as follows in the native complex: TM1 (cyan), TM2 (pink), TM3 (magenta), TM4 (cyan), TM5 (orange), TM6 (green), and TM7 (blue). Key interacting residues are highlighted and labeled in each structure. The ECLs are color-coded in nAT1R- SDBPA as cyan and in mAT1R- SDBPA as yellow. The n-terminal as brown color.

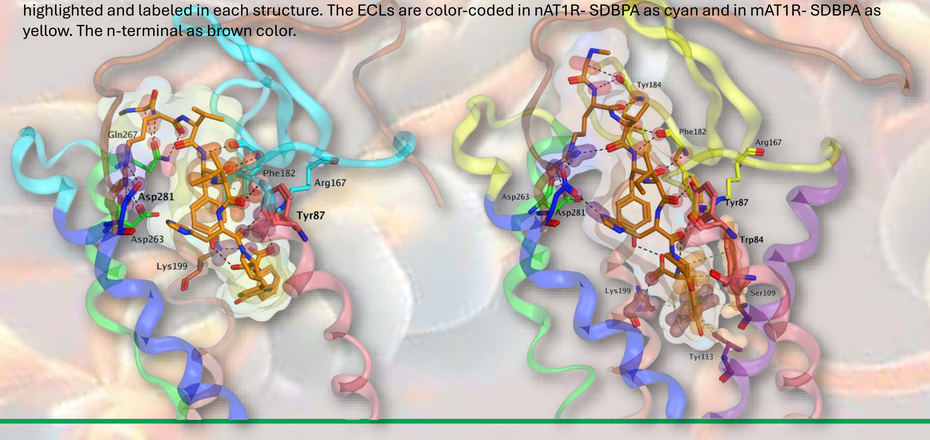

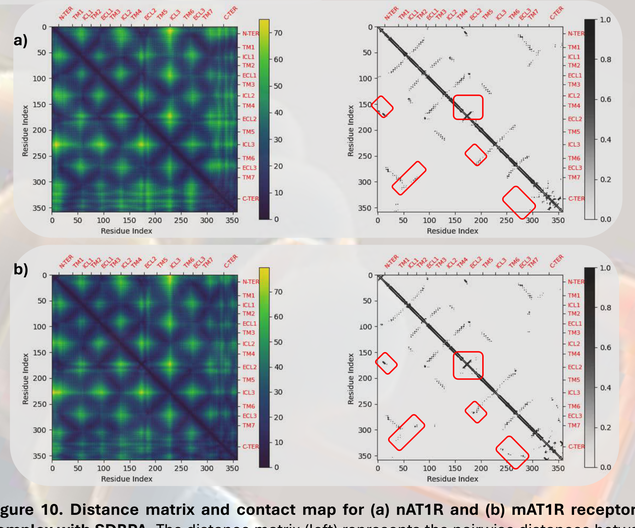

Figure 10. Distance matrix and contact map for (a) nAT1R and (b) mAT1R receptor in complex with SDBPA. The distance matrix (left) represents the pairwise distances between residues, with color intensity indicating the distance magnitude (dark purple: short distance, yellow: long distance). The contact map (right) shows binary contacts between residues based on a threshold distance of 8 Å (black: contact, white: no contact). Red boxes highlight specific domains and their interaction patterns with other residues in the protein.

CONCLUSION & PERSPECTIVES

This study proposes that there exist significant interactions between the mutant W253A-AT1R and specific determinants of the different peptide ligands, which are involved in stabilizing the receptor in a conformation capable of recognizing β-arrestin. To investigate the structural dynamics of the native AT1R and W253A-AT1R mutant receptor, we utilized 1 microsecond molecular dynamics (MD) simulations. Our study incorporated interactions with the native endogenous ligand and the three modified peptides. Our simulations revealed distinct conformational landscapes for each receptor-ligand pairing, with particular emphasis on regions of flexibility and interaction. Significantly, these unique conformational tendencies, lead to a better understanding of the molecular determinants responsible for selecting a given biased pathway. This information provides opportunities to design biased agonists with great therapeutic promise, as they may offer the potential for enhanced efficacy and reduced side effects.

References:
1. Van Haaster, McDonough, Gurley, Curr Opin Nephrol Hypertens, 2018, 27, 1-7.
2. Wingler, Skiba, McMahon, Staus, Kleinhenz, Suomivuori, Latorraca, Dror, Lefkowitz, Kruse, 2020,367, 888-892.

Acuité Québec
INSTITUT DE PHARMACOLOGIE DE SHERBROOKE UdeS
BINDREAULT
NSERC CRSNG
IRSC CIHR